



INTERNATIONAL CENTRE FOR THEORETICAL PHYSICS

UNITARIZATION OF KÖRNER-KURODA MODEL OF ELECTROMAGNETIC STRUCTURE OF OCTET $1/2^+$ BARYONS

Stanislav Dubnička

Anna Zuzana Dubničková

Jerzy Kraskiewicz

and

Ryszard Raczka



INTERNATIONAL
ATOMIC ENERGY
AGENCY



UNITED NATIONS
EDUCATIONAL,
SCIENTIFIC
AND CULTURAL
ORGANIZATION

MIRAMARE-TRIESTE



International Atomic Energy Agency
and
United Nations Educational Scientific and Cultural Organization
INTERNATIONAL CENTRE FOR THEORETICAL PHYSICS

UNITARIZATION OF KÖRNER-KURODA MODEL
OF ELECTROMAGNETIC STRUCTURE OF OCTET $1/2^+$ BARYONS

Stanislav Dubnička¹,
International Centre for Theoretical Physics, Trieste, Italy,

Anna Zuzana Dubničková
Department of Theoretical Physics, Comenius University,
Mlynská dolina, 842 15 Bratislava, Slovakia

and

Jerzy Kraskiewicz² and Ryszard Raczyński³
Scuola Internazionale Superiore di Studi Avanzati (SISSA), Trieste, Italy.

ABSTRACT

The Körner-Kuroda model of the electromagnetic structure of octet $1/2^+$ baryons is restored on a more topical physical basis. Electromagnetic radii of baryons under consideration are calculated and compared with other model predictions. By an incorporation of a two-cut approximation of correct form factor analytic properties and nonzero vector-meson widths, the Körner-Kuroda model is unitarized, providing in this manner imaginary parts of the octet $1/2^+$ baryon form factors to be nonzero just starting from a branch point corresponding to the lowest threshold.

MIRAMARE - TRIESTE

October 1994

¹On leave of absence from: Institute of Physics, Slovak Academy of Sciences, Dúbravská cesta, 842 15 Bratislava, Slovakia.

²On leave of absence from: Maria Skłodowska-Curie University, ul. Radziszewskiego 10, 20031 Lublin, Poland.

³On leave of absence from: Soltan Institute for Nuclear Studies, ul. Hoza 69, 00681 Warsaw, Poland.

1 INTRODUCTION

Though there is approximately 40 years from the discovery of the electromagnetic (EM) structure of hadrons, a knowledge about the EM structure of octet $1/2^+$ baryons is unsatisfactory up to now. Almost all experimental investigations are concentrated to the proton [1,2] and mainly in the space-like region [1]. Less precise information exists on neutron [1,3]. Concerning other members of the baryon $1/2^+$ octet, there is only one experimental point on the total cross section of the $\Lambda\bar{\Lambda}$ production in e^+e^- annihilation and an upper limit on the cross-section of the $\Sigma^0\bar{\Sigma}^0$ production at $t=5.693$ GeV² [4]. There is no experimental information on the electromagnetic structure of Σ^\pm and Ξ -hyperons up to now.

Inspired by a good experimental situation, many more or less successful phenomenological models [5-14] have been constructed for a global description of the nucleon EM structure. However, missing are analogous attempts to predict the behaviour of EM form factors (FF) of other baryons of the same octet. The main reason is that almost all constructed models depend on some number of free parameters which, however, have to be fixed in a comparison with experimental data. Possibly, exceptions are a calculation [15] of the EM FF's of the Λ^0 - and Σ^0 -hyperons in the space-like region using a relativised constituent quark model, which includes correction terms related to the potential acting between the quarks and to the center-of-mass motion during the photon baryon scattering. Then also a global reproduction [16] of Λ^0 -hyperon EM FF's was carried out in the framework of the simplified unitary and analytic model and the Körner-Kuroda zero vector-meson width model [17] (and therefore real in both, the space-like and also in the time-like region) of the EM structure of octet $1/2^+$ baryons with the correct asymptotic behaviour does exist. The latter was used (see [17]) for a prediction of total cross-sections of electron-positron annihilation into baryon-antibaryon pair which depends on absolute values of EM FF's of baryons. However, for an investigation of polarization effects [18-20], where in the corresponding cross-sections real and imaginary part of a product of electric and magnetic FF's in $t > 4m_B^2$ region appear, the Körner-Kuroda model is no more applicable. The main reason is, that EM FF's in time-like region for $t > t_0$, where t_0 is the lowest normal or anomalous threshold, are complex functions with a phase dependent on energy and the Körner-Kuroda model gives only the phase to be zero up to $+\infty$. However, as the Körner-Kuroda model is one of the first models for EM FF's of all members of $1/2^+$ octet, by using an effective method proposed in the paper [14] we unitarize the Körner-Kuroda model, providing in such manner baryon FF's suitable for an investigation of polarization effects in annihilation channels.

Our paper is organized as follows. In the next section we restore the Körner-Kuroda model on a more topical physical basis. Then, since much progress has been achieved in understanding the static EM properties of the octet $1/2^+$ baryons, directly connected with a behaviour of EM FF's around $t = 0$, we calculate by means of the Körner-Kuroda zero vector-meson width model EM radii and compare them with predictions of other models, like quark models [15,21,22], Skyrme model [23], lattice QCD approach [24], naive VMD model [25] and extended VMD model constrained by QCD asymptotics [26]. The section

3 is devoted to the unitarization of the Körner-Kuroda model and to predictions of a behaviour of total cross-sections of electron-positron annihilation into baryon-antibaryon pair. In conclusions the main results of our paper are summarized.

2 KÖRNER-KURODA MODEL OF THE EM FORM FACTORS OF OCTET $1/2^+$ BARYONS

The EM structure of every baryon of $1/2^+$ octet is completely described by two scalar functions depending on the four momentum transfer squared $t = -Q^2$. In accordance with [17] they are chosen in the form of the Sachs electric $G_E(t)$ and magnetic $G_M(t)$ FF's [27], which can be expressed through Dirac $F_1(t)$ and Pauli $F_2(t)$ FF's as follows

$$\begin{aligned} G_E(t) &= F_1(t) + \frac{t}{4m_B^2} F_2(t) \\ G_M(t) &= F_1(t) + F_2(t), \end{aligned} \quad (1)$$

where m_B is the mass of a corresponding baryon. All those FF's are normalized in the following way

$$\begin{aligned} G_E(0) &= Q_B; & F_1(0) &= Q_B; \\ G_M(0) &= Q_B + \mu_B; & F_2(0) &= \mu_B, \end{aligned} \quad (2)$$

where Q_B and μ_B are the charge and anomalous magnetic moment of the baryon, respectively.

Now, for a decomposition of $F_1(t)$ and $F_2(t)$ into various vector-meson family contributions, we use the Körner-Kuroda tabulated values of relative ρ -, ω - and ϕ - family couplings to the baryon-antibaryon system [17]

$$\begin{aligned} F_{1p}(t) &= \frac{1}{2} F_{1p}^\rho + \frac{1}{2} F_{1p}^\omega \\ F_{2p}(t) &= \left(\frac{1}{3} + \frac{5}{6}\mu_p\right) F_{2p}^\rho + \left(-\frac{1}{3} + \frac{1}{6}\mu_p\right) F_{2p}^\omega \end{aligned} \quad (3)$$

$$\begin{aligned} F_{1n}(t) &= -\frac{1}{2} F_{1n}^\rho + \frac{1}{2} F_{1n}^\omega \\ F_{2n}(t) &= -\left(\frac{1}{3} + \frac{5}{6}\mu_n\right) F_{2n}^\rho + \left(-\frac{1}{3} + \frac{1}{6}\mu_n\right) F_{2n}^\omega \end{aligned} \quad (4)$$

$$\begin{aligned} F_{1\Lambda}(t) &= \frac{1}{3} F_{1\Lambda}^\omega - \frac{1}{3} F_{1\Lambda}^\phi \\ F_{2\Lambda}(t) &= -\frac{1}{3} F_{2\Lambda}^\omega - \frac{1}{3} \mu_p F_{1\Lambda}^\phi \end{aligned} \quad (5)$$

$$\begin{aligned} F_{1\Sigma^+}(t) &= F_{1\Sigma^+}^\rho + \frac{1}{3} F_{1\Sigma^+}^\omega - \frac{1}{3} F_{1\Sigma^+}^\phi \\ F_{2\Sigma^+}(t) &= -\left(\frac{1}{3} - \frac{2}{3}\mu_p\right) F_{2\Sigma^+}^\rho + \left(-\frac{1}{9} + \frac{2}{9}\mu_p\right) F_{2\Sigma^+}^\omega + \left(\frac{4}{9} + \frac{1}{9}\mu_p\right) F_{2\Sigma^+}^\phi \end{aligned} \quad (6)$$

$$\begin{aligned} F_{1\Sigma^0}(t) &= \frac{1}{3} F_{1\Sigma^0}^\omega - \frac{1}{3} F_{1\Sigma^0}^\phi \\ F_{2\Sigma^0}(t) &= \left(-\frac{1}{9} + \frac{2}{9}\mu_p\right) F_{2\Sigma^0}^\omega + \left(\frac{4}{9} + \frac{1}{9}\mu_p\right) F_{2\Sigma^0}^\phi \end{aligned} \quad (7)$$

$$\begin{aligned} F_{1\Sigma^-}(t) &= -F_{1\Sigma^-}^\rho + \frac{1}{3} F_{1\Sigma^-}^\omega - \frac{1}{3} F_{1\Sigma^-}^\phi \\ F_{2\Sigma^-}(t) &= \left(\frac{1}{3} - \frac{2}{3}\mu_p\right) F_{2\Sigma^-}^\rho + \left(-\frac{1}{9} + \frac{2}{9}\mu_p\right) F_{2\Sigma^-}^\omega + \left(\frac{4}{9} + \frac{1}{9}\mu_p\right) F_{2\Sigma^-}^\phi \end{aligned} \quad (8)$$

$$\begin{aligned} F_{1\Sigma^0}(t) &= \frac{1}{2} F_{1\Sigma^0}^\rho + \frac{1}{6} F_{1\Sigma^0}^\omega - \frac{2}{3} F_{1\Sigma^0}^\phi \\ F_{2\Sigma^0}(t) &= -\left(\frac{2}{3} + \frac{1}{6}\mu_p\right) F_{2\Sigma^0}^\rho + \left(-\frac{2}{9} - \frac{1}{18}\mu_p\right) F_{2\Sigma^0}^\omega + \left(\frac{2}{9} - \frac{4}{9}\mu_p\right) F_{2\Sigma^0}^\phi \end{aligned} \quad (9)$$

$$\begin{aligned} F_{1\Sigma^-}(t) &= -\frac{1}{2} F_{1\Sigma^-}^\rho + \frac{1}{6} F_{1\Sigma^-}^\omega - \frac{2}{3} F_{1\Sigma^-}^\phi \\ F_{2\Sigma^-}(t) &= \left(\frac{2}{3} + \frac{1}{6}\mu_p\right) F_{2\Sigma^-}^\rho + \left(-\frac{2}{9} - \frac{1}{18}\mu_p\right) F_{2\Sigma^-}^\omega + \left(\frac{2}{9} - \frac{4}{9}\mu_p\right) F_{2\Sigma^-}^\phi \end{aligned} \quad (10)$$

which automatically respect the normalizations (2) provided

$$F_{1B}^v(t)|_{t=0} = F_{2B}^v(t)|_{t=0} = 1 \text{ where } B = p, n, \Lambda, \Sigma^+, \Sigma^0, \Sigma^-, \Xi^0, \Xi^-; \quad (11)$$

$$v = \rho, \omega, \phi$$

and also transformation properties of the baryon EM current under rotations in isotopic space. Just in order to conserve the latter symmetry (a change of the sign in the ρ -contribution from p to n , from Σ^+ to Σ^- and from Ξ^0 to Ξ^-) we do not employ in this paper experimental values of magnetic moments of baryons, but we take them to be SU(6) values related to the magnetic moment of the proton, like in [17].

It is well known that the perturbative QCD predicts [28,29] the asymptotic behaviour $G_E(t)$ and $G_M(t)$ to be (up to logarithmic corrections)

$$G_E(t)|_{|t|\rightarrow\infty} \rightarrow t^{-2}; \quad G_M(t)|_{|t|\rightarrow\infty} \rightarrow t^{-2}; \quad (12)$$

from where it is natural to deduce the asymptotic behavior of $F_1(t)$ and $F_2(t)$ as follows

$$F_1(t)|_{|t|\rightarrow\infty} \rightarrow t^{-2}; \quad F_2(t)|_{|t|\rightarrow\infty} \rightarrow t^{-3}. \quad (13)$$

In order to satisfy (13) we assume that all F_{1B}^v and F_{2B}^v in (3)-(10) behave like

$$F_{1B}^v(t)|_{|t|\rightarrow\infty} \rightarrow t^{-2}; \quad F_{2B}^v(t)|_{|t|\rightarrow\infty} \rightarrow t^{-3}. \quad (14)$$

Then, parametrizing F_{1B}^v and F_{2B}^v by means of the vector-meson dominance (VMD) model, we are restricted always with two and three vector mesons, respectively, as follows

$$F_{1B}^v = \sum_{i=v}^{v'} \frac{m_i^2}{m_i^2 - t} (f_{iBB}^{(1)}/f_i); \quad F_{2B}^v = \sum_{i=v}^{v''} \frac{m_i^2}{m_i^2 - t} (f_{iBB}^{(2)}/f_i), \quad (15)$$

where m_i are masses of vector mesons with quantum numbers of the photon, v' and v'' are the first and the second excited state of vector meson v , f_{iBB} is the coupling constant of the vector meson to baryon and f_i is the so-called universal vector meson coupling constant describing the transition between the virtual photon and the vector meson.

If we transform relations (15) in order to have common denominator, then requiring normalizations (11) and the asymptotic behaviour (14), we come to the following two systems of closed algebraic equations

$$(f_{vBB}^{(1)}/f_v) + (f_{v'BB}^{(1)}/f_{v'}) = 1 \quad (16)$$

$$m_v^2(f_{vBB}^{(1)}/f_v) + m_{v'}^2(f_{v'BB}^{(1)}/f_{v'}) = 0$$

$$(f_{vBB}^{(2)}/f_v) + (f_{v'BB}^{(2)}/f_{v'}) + (f_{v''BB}^{(2)}/f_{v''}) = 1$$

$$m_v^2(f_{vBB}^{(2)}/f_v) + m_{v'}^2(f_{v'BB}^{(2)}/f_{v'}) + m_{v''}^2(f_{v''BB}^{(2)}/f_{v''}) = 0 \quad (17)$$

$$m_v^2(m_v^2 + m_{v''}^2)(f_{vBB}^{(2)}/f_v) + m_{v'}^2(m_v^2 + m_{v''}^2)(f_{v'BB}^{(2)}/f_{v'}) + m_{v''}^2(m_v^2 + m_{v''}^2)(f_{v''BB}^{(2)}/f_{v''}) = 0$$

and by their solutions, to the expressions as follows

$$F_{1B}^v = \frac{m_v^2 m_{v''}^2}{(m_v^2 - t)(m_{v''}^2 - t)}; \quad F_{2B}^v = \frac{m_v^2 m_{v'}^2 m_{v''}^2}{(m_v^2 - t)(m_{v'}^2 - t)(m_{v''}^2 - t)}. \quad (18)$$

Finally, substituting relations (18) into (3)-(10) we find just the representation of the Dirac and Pauli FF's of baryons to be identical with the form presented in [17].

As we have mentioned in the Introduction, much progress has been achieved in understanding of the static EM properties of the octet $1/2^+$ baryons, including the electromagnetic radii. Therefore it is interesting to calculate the latter in the framework of the Körner-Kuroda zero vector-meson width model and to compare them with other model predictions.

The electric and magnetic mean-square radius of any baryon can be extracted from the corresponding electric and magnetic FF's with the standard small t expansion of the Fourier transform of a charge or magnetic moment distribution by

$$\langle r_E^2 \rangle = 6 \cdot \frac{dG_E(t)}{dt} \Big|_{t=0}; \quad \langle r_M^2 \rangle = 6 \cdot \frac{dG_M(t)}{dt} \Big|_{t=0} \quad (19)$$

respectively. Applying them to the octet $1/2^+$ baryon EM FF's one gets the electric and magnetic mean-square radii of baryons in the following form

$$\begin{aligned} \langle r_{E_p}^2 \rangle &= 3(D_{1\rho} + D_{1\omega} + \mu_p/2m_p^2) \\ \langle r_{M_p}^2 \rangle &= 3(D_{1\rho} + D_{1\omega}) + (2 + 5\mu_p)D_{2\rho} + (-2 + \mu_p)D_{2\omega} \end{aligned} \quad (20)$$

$$\begin{aligned} \langle r_{E_n}^2 \rangle &= -3(D_{1\rho} - D_{1\omega}) - (1 + \mu_p)/2m_n^2 \\ \langle r_{M_n}^2 \rangle &= -3(D_{1\rho} - D_{1\omega}) - (2 + 5\mu_p)D_{2\rho} + (-2 + \mu_p)D_{2\omega} \end{aligned} \quad (21)$$

$$\begin{aligned} \langle r_{E_\Lambda}^2 \rangle &= 2(D_{1\omega} - D_{1\phi}) - (1 + \mu_p)/2m_\Lambda^2 \\ \langle r_{M_\Lambda}^2 \rangle &= 2(D_{1\omega} - D_{1\phi} - D_{2\omega} - \mu_p D_{2\phi}) \end{aligned} \quad (22)$$

$$\begin{aligned} \langle r_{E_{\Sigma^+}}^2 \rangle &= 6D_{1\rho} + 2(D_{1\omega} - D_{1\phi}) + 3\mu_p/2m_{\Sigma^+}^2 \\ \langle r_{M_{\Sigma^+}}^2 \rangle &= 6D_{1\rho} + 2(D_{1\omega} - D_{1\phi}) - (2 - 4\mu_p)D_{2\rho} + (-\frac{2}{3} + \frac{4}{3}\mu_p)D_{2\omega} + (\frac{8}{3} + \frac{2}{3}\mu_p)D_{2\phi} \end{aligned} \quad (23)$$

$$\begin{aligned} \langle r_{E_{\Sigma^0}}^2 \rangle &= 2(D_{1\omega} - D_{1\phi}) + (1 + \mu_p)/2m_{\Sigma^0}^2 \\ \langle r_{M_{\Sigma^0}}^2 \rangle &= 2(D_{1\omega} - D_{1\phi}) + (-\frac{2}{3} + \frac{4}{3}\mu_p)D_{2\omega} + (\frac{8}{3} + \frac{2}{3}\mu_p)D_{2\phi} \end{aligned} \quad (24)$$

$$\begin{aligned} \langle r_{E_{\Sigma^-}}^2 \rangle &= -6D_{1\rho} + 2(D_{1\omega} - D_{1\phi}) + (2 - \mu_p)/2m_{\Sigma^-}^2 \\ \langle r_{M_{\Sigma^-}}^2 \rangle &= -6D_{1\rho} + 2(D_{1\omega} - D_{1\phi}) - 2(1 - 2\mu_p)D_{2\rho} + (-\frac{2}{3} + \frac{4}{3}\mu_p)D_{2\omega} + (\frac{8}{3} + \frac{2}{3}\mu_p)D_{2\phi} \end{aligned} \quad (25)$$

$$\begin{aligned} \langle r_{E_{\Xi^0}}^2 \rangle &= 3D_{1\rho} + D_{1\omega} - 4D_{1\phi} - (1 + \mu_p)/m_{\Xi^0}^2 \\ \langle r_{M_{\Xi^0}}^2 \rangle &= 3D_{1\rho} + D_{1\omega} - 4D_{1\phi} - (4 + \mu_p)D_{2\rho} - (\frac{4}{3} + \frac{1}{3}\mu_p)D_{2\omega} + (\frac{4}{3} - \frac{8}{3}\mu_p)D_{2\phi} \end{aligned} \quad (26)$$

$$\begin{aligned} \langle r_{E_{\Xi^-}}^2 \rangle &= -3D_{1\rho} + D_{1\omega} - 4D_{1\phi} + (2 - \mu_p)/2m_{\Xi^-}^2 \\ \langle r_{M_{\Xi^-}}^2 \rangle &= -3D_{1\rho} + D_{1\omega} - 4D_{1\phi} + (4 + \mu_p)D_{2\rho} - (\frac{4}{3} + \frac{1}{3}\mu_p)D_{2\omega} + (\frac{4}{3} - \frac{8}{3}\mu_p)D_{2\phi}, \end{aligned} \quad (27)$$

where

$$D_{1v} = \sum_{i=v}^{v'} \frac{1}{m_i^2}; \quad D_{2v} = \sum_{i=v}^{v''} \frac{1}{m_i^2}; \quad v = \rho, \omega, \phi. \quad (28)$$

In order to get numerical values from (20)-(27), unlike the paper [17], where the masses of excited states are determined by means of slopes of Regge trajectories, here we take the existing experimental values of all the vector meson masses, given by the Rev. of Particle Properties [30]. There is, however, an experimental confirmation only of one of the excited states of $\phi(1020)$ -meson. Therefore the mass of the second one was estimated by means of the Gell-Mann-Okubo mass formula [31]

$$4m_{K^*}^2 = m_\rho^2 + 3m_\phi^2 \cos^2 \vartheta + 3m_\omega^2 \sin^2 \vartheta \quad (29)$$

considering an ideal $\phi - \omega$ mixing i.e. taking $\cos \vartheta = \sqrt{2/3}$ and $\sin \vartheta = \sqrt{1/3}$.

Here we would like to note, that just from (29) one can know the experimentally confirmed $\phi(1680)$ -meson to be the second excited state of $\phi(1020)$ -meson and the first one can be expected with the mass $m_{\phi'} \approx 1.4$ GeV.

The predicted values of electric and magnetic mean-square radii by the Körner-Kuroda model are presented in Table 1 and Table 2, where they are compared also with other model predictions, like the lattice QCD [24], nonrelativistic [21,22] and relativistic [15] quark models, Skyrme model [23], naive VMD model combined with SU(3) symmetry [25] and the extended VMD model constrained by QCD asymptotics. They are quite encouraging and at the same time they support reliability of the Körner-Kuroda model, at least around the point $t = 0$.

3 UNITARIZATION OF KÖRNER-KURODA MODEL

The main aim of this paper is the unitarization of the Körner-Kuroda zero vector-meson width model, restored in the previous section, in order to provide in such manner octet $1/2^+$ baryon FF's suitable for an investigation of polarization effects in annihilation channels. For the latter an effective method developed in paper [14] for nucleons will be used.

There is a general belief (in some cases proved in the framework of the axiomatic quantum field theory, but always restored from the Feynmann diagrams of a formal perturbation expansion) that the octet $1/2^+$ baryon EM FF's are analytic in the whole complex plane of t , besides the cut starting from the lowest branch point t_0 on the real axis up to $+\infty$. From the physical point of view, the unitarity condition requires the imaginary part of the octet $1/2^+$ baryon FF's to be different from zero just above the

lowest branch point t_0 and, moreover, it determines a smoothly varying behaviour of the imaginary part in the $t_0 < t < \infty$ region.

For $t < t_0$ the baryon EM FF imaginary part is equal to zero as a consequence of the hermiticity of the EM current.

All these properties are not contained in the Körner-Kuroda zero vector-meson width model given by (1), (3)-(10) and (18).

The unitarization of the Körner-Kuroda model is achieved by the incorporation of the correct FF analytic properties and non-zero values of vector meson widths into the expressions (18). Here we have to distinguish the isovector (ρ -meson) vector-meson family contributions from the isoscalar (ω - and ϕ -meson) vector meson contributions, because in the isoscalar case the lowest normal threshold is given by $t_0^* = 9m_\pi^2$ and in the isovector case the lowest normal threshold is at $t_0^* = 4m_\pi^2$, where m_π is the pion mass. So, practically the unitarization of Körner-Kuroda model is realized (up to the two-cut approximation) by the following special nonlinear transformations

$$\begin{aligned} t &= t_0^* - \frac{4(t_{in}^B - t_0^*)}{[1/V - V]^2} \\ t &= t_0^* - \frac{4(t_{in}^B - t_0^*)}{[1/W - W]^2} \end{aligned} \quad (30)$$

applied to (18), where t_0^* , t_0^v and $t_{in}^B = 4m_B^2$ are square-root branch points. The latter is transparent from the inverse transformation

$$V(t) = i \frac{[(t_{in}^B/t_0^* - 1)^{1/2} + (t/t_0^* - 1)^{1/2}]^{1/2} - [(t_{in}^B/t_0^* - 1)^{1/2} - (t/t_0^* - 1)^{1/2}]^{1/2}}{[(t_{in}^B/t_0^* - 1)^{1/2} + (t/t_0^* - 1)^{1/2}]^{1/2} + [(t_{in}^B/t_0^* - 1)^{1/2} - (t/t_0^* - 1)^{1/2}]^{1/2}} \quad (31)$$

and similarly for $W(t)$.

Practically, in the incorporation of the two-cut approximation of the octet $1/2^+$ baryon FF analytic properties into (18), besides (30), we also use expressions for vector meson masses squared

$$m_s^2 = t_0^* - \frac{4(t_{in}^B - t_0^*)}{[1/V_{s0} - V_{s0}]^2}; \quad m_v^2 = t_0^v - \frac{4(t_{in}^B - t_0^*)}{[1/W_{v0} - W_{v0}]^2} \quad (32)$$

and identities

$$0 = t_0^* - \frac{4(t_{in}^B - t_0^*)}{[1/V_N - V_N]^2}; \quad 0 = t_0^v - \frac{4(t_{in}^B - t_0^*)}{[1/W_N - W_N]^2} \quad (33)$$

following from (30), where V_{s0} , W_{v0} are the zero-width (that is why they have a subindex 0) VMD poles and V_N , W_N are the normalization points (corresponding to $t = 0$) in the V , W planes, respectively. Relations (30), (32) and (33) first transform every VMD term $m_s^2/(m_s^2 - t)$ into the corresponding new variable as follows

$$\frac{m_s^2 - 0}{m_s^2 - t} = \left(\frac{1 - W^2}{1 - W_N^2} \right)^2 \cdot \frac{(W_N - W_{v0})(W_N + W_{v0})(W_N - 1/W_{v0})(W_N + 1/W_{v0})}{(W - W_{v0})(W + W_{v0})(W - 1/W_{v0})(W + 1/W_{v0})}. \quad (34)$$

Then, utilizing the relation between complex and complex conjugate values of the corresponding zero-width VMD pole positions in the V , W planes

$$V_{s0} = -V_{s0}^* \quad W_{v0} = -W_{v0}^* \quad (35)$$

following from the fact that all $(m_v^2 - \Gamma_v^2/4) < t_{in}^B$, and subsequently incorporating the non-zero values of vector meson width $\Gamma \neq 0$ in a correct way, one gets for every octet $1/2^+$ baryon EM FF, one analytic function in the whole complex t -plane besides two right-hand cuts of the following form

$$F_{1\rho}(t) = \frac{1}{2} \left\{ \left(\frac{1 - W_\rho^2}{1 - W_{\rho N}^2} \right)^4 \prod_{i=\rho}^{\rho'} U_i^{\rho'} [W_\rho(t)] + \left(\frac{1 - V_\rho^2}{1 - V_{\rho N}^2} \right)^4 \prod_{i=\omega}^{\omega'} R_i^{\rho'} [V_\rho(t)] \right\} \quad (36)$$

$$F_{2\rho}(t) = \left(\frac{1}{3} + \frac{5}{6}\mu_\rho \right) \left(\frac{1 - W_\rho^2}{1 - W_{\rho N}^2} \right)^6 \prod_{i=\rho}^{\rho''} U_i^{\rho''} [W_\rho(t)] + \left(-\frac{1}{3} + \frac{1}{6}\mu_\rho \right) \left(\frac{1 - V_\rho^2}{1 - V_{\rho N}^2} \right)^6 \prod_{i=\omega}^{\omega''} R_i^{\rho''} [V_\rho(t)]$$

$$F_{1n}(t) = -\frac{1}{2} \left\{ \left(\frac{1 - W_n^2}{1 - W_{nN}^2} \right)^4 \prod_{i=\rho}^{\rho'} U_i^{\rho'} [W_n(t)] - \left(\frac{1 - V_n^2}{1 - V_{nN}^2} \right)^4 \prod_{i=\omega}^{\omega'} R_i^{\rho'} [V_n(t)] \right\} \quad (37)$$

$$F_{2n}(t) = -\left(\frac{1}{3} + \frac{5}{6}\mu_\rho \right) \left(\frac{1 - W_n^2}{1 - W_{nN}^2} \right)^6 \prod_{i=\rho}^{\rho''} U_i^{\rho''} [W_n(t)] + \left(-\frac{1}{3} + \frac{1}{6}\mu_\rho \right) \left(\frac{1 - V_n^2}{1 - V_{nN}^2} \right)^6 \prod_{i=\omega}^{\omega''} R_i^{\rho''} [V_n(t)]$$

$$F_{1\Lambda}(t) = \frac{1}{3} \left\{ \left(\frac{1 - V_\Lambda^2}{1 - V_{\Lambda N}^2} \right)^4 \prod_{i=\omega}^{\omega'} R_i^{\Lambda'} [V_\Lambda(t)] - \prod_{i=\phi}^{\phi'} R_i^{\Lambda'} [V_\Lambda(t)] \right\} \quad (38)$$

$$F_{2\Lambda}(t) = -\frac{1}{3} \left\{ \left(\frac{1 - V_\Lambda^2}{1 - V_{\Lambda N}^2} \right)^6 \prod_{i=\omega}^{\omega''} R_i^{\Lambda''} [V_\Lambda(t)] + \mu_\rho \prod_{i=\phi}^{\phi''} R_i^{\Lambda''} [V_\Lambda(t)] \right\}$$

$$F_{1\Sigma^+}(t) = \left(\frac{1 - W_{\Sigma^+}^2}{1 - W_{\Sigma^+ N}^2} \right)^4 \prod_{i=\rho}^{\rho'} U_i^{\Sigma^+} [W_{\Sigma^+}(t)] + \frac{1}{3} \left(\frac{1 - V_{\Sigma^+}^2}{1 - V_{\Sigma^+ N}^2} \right)^4 \left\{ \prod_{i=\omega}^{\omega'} R_i^{\Sigma^+} [V_{\Sigma^+}(t)] - \prod_{i=\phi}^{\phi'} R_i^{\Sigma^+} [V_{\Sigma^+}(t)] \right\}$$

$$F_{2\Sigma^+}(t) = -\left(\frac{1}{3} - \frac{2}{3}\mu_\rho \right) \left(\frac{1 - W_{\Sigma^+}^2}{1 - W_{\Sigma^+ N}^2} \right)^6 \prod_{i=\rho}^{\rho''} U_i^{\Sigma^+} [W_{\Sigma^+}(t)] + \left(\frac{1 - V_{\Sigma^+}^2}{1 - V_{\Sigma^+ N}^2} \right)^6 \left\{ \left(-\frac{1}{9} + \frac{2}{9}\mu_\rho \right) \prod_{i=\omega}^{\omega''} R_i^{\Sigma^+} [V_{\Sigma^+}(t)] + \left(\frac{4}{9} + \frac{1}{9}\mu_\rho \right) \prod_{i=\phi}^{\phi''} R_i^{\Sigma^+} [V_{\Sigma^+}(t)] \right\} \quad (39)$$

$$F_{1\Sigma^0}(t) = \frac{1}{3} \left\{ \left(\frac{1 - V_{\Sigma^0}^2}{1 - V_{\Sigma^0 N}^2} \right)^4 \prod_{i=\omega}^{\omega'} R_i^{\Sigma^0} [V_{\Sigma^0}(t)] - \prod_{i=\phi}^{\phi'} R_i^{\Sigma^0} [V_{\Sigma^0}(t)] \right\} \quad (40)$$

$$F_{2\Sigma^0}(t) = \left(\frac{1 - V_{\Sigma^0}^2}{1 - V_{\Sigma^0 N}^2} \right)^6 \left\{ \left(-\frac{1}{9} + \frac{2}{9}\mu_\rho \right) \prod_{i=\omega}^{\omega''} R_i^{\Sigma^0} [V_{\Sigma^0}(t)] + \left(\frac{4}{9} + \frac{1}{9}\mu_\rho \right) \prod_{i=\phi}^{\phi''} R_i^{\Sigma^0} [V_{\Sigma^0}(t)] \right\}$$

$$\begin{aligned}
F_{1\Sigma^-}(t) &= -\left(\frac{1-W_{\Sigma^-}^2}{1-W_{\Sigma^-N}^2}\right)^4 \prod_{i=\rho}^{\rho'} U_i^{\Sigma^-}[W_{\Sigma^-}(t)] + \\
&+ \frac{1}{3} \left(\frac{1-V_{\Sigma^-}^2}{1-V_{\Sigma^-N}^2}\right)^4 \left\{ \prod_{i=\omega}^{\omega'} R_i^{\Sigma^-}[V_{\Sigma^-}(t)] - \prod_{i=\phi}^{\phi'} R_i^{\Sigma^-}[V_{\Sigma^-}(t)] \right\} \\
F_{2\Sigma^-}(t) &= \left(\frac{1}{3} - \frac{2}{3}\mu_p\right) \left(\frac{1-W_{\Sigma^-}^2}{1-W_{\Sigma^-N}^2}\right)^6 \prod_{i=\rho}^{\rho''} U_i^{\Sigma^-}[W_{\Sigma^-}(t)] + \\
&+ \left(\frac{1-V_{\Sigma^-}^2}{1-V_{\Sigma^-N}^2}\right)^6 \left\{ \left(-\frac{1}{9} + \frac{2}{9}\mu_p\right) \prod_{i=\omega}^{\omega''} R_i^{\Sigma^-}[V_{\Sigma^-}(t)] + \left(\frac{4}{9} + \frac{1}{9}\mu_p\right) \prod_{i=\phi}^{\phi''} R_i^{\Sigma^-}[V_{\Sigma^-}(t)] \right\}
\end{aligned} \tag{41}$$

$$\begin{aligned}
F_{1\Sigma^0}(t) &= \frac{1}{2} \left(\frac{1-W_{\Sigma^0}^2}{1-W_{\Sigma^0N}^2}\right)^4 \prod_{i=\rho}^{\rho'} U_i^{\Sigma^0}[W_{\Sigma^0}(t)] + \left(\frac{1-V_{\Sigma^0}^2}{1-V_{\Sigma^0N}^2}\right)^4 \left\{ \frac{1}{6} \prod_{i=\omega}^{\omega'} R_i^{\Sigma^0}[V_{\Sigma^0}(t)] - \right. \\
&\left. - \frac{2}{3} \prod_{i=\phi}^{\phi'} R_i^{\Sigma^0}[V_{\Sigma^0}(t)] \right\} \\
F_{2\Sigma^0}(t) &= -\left(\frac{2}{3} + \frac{1}{6}\mu_p\right) \left(\frac{1-W_{\Sigma^0}^2}{1-W_{\Sigma^0N}^2}\right)^6 \prod_{i=\rho}^{\rho''} U_i^{\Sigma^0}[W_{\Sigma^0}(t)] + \\
&+ \left(\frac{1-V_{\Sigma^0}^2}{1-V_{\Sigma^0N}^2}\right)^6 \left\{ \left(-\frac{2}{9} - \frac{1}{18}\mu_p\right) \prod_{i=\omega}^{\omega''} R_i^{\Sigma^0}[V_{\Sigma^0}(t)] + \left(\frac{2}{9} - \frac{4}{9}\mu_p\right) \prod_{i=\phi}^{\phi''} R_i^{\Sigma^0}[V_{\Sigma^0}(t)] \right\}
\end{aligned} \tag{42}$$

$$\begin{aligned}
F_{1\Sigma^-}(t) &= -\frac{1}{2} \left(\frac{1-W_{\Sigma^-}^2}{1-W_{\Sigma^-N}^2}\right)^4 \prod_{i=\rho}^{\rho'} U_i^{\Sigma^-}[W_{\Sigma^-}(t)] + \left(\frac{1-V_{\Sigma^-}^2}{1-V_{\Sigma^-N}^2}\right)^4 \left\{ \frac{1}{6} \prod_{i=\omega}^{\omega'} R_i^{\Sigma^-}[V_{\Sigma^-}(t)] - \right. \\
&\left. - \frac{2}{3} \prod_{i=\phi}^{\phi'} R_i^{\Sigma^-}[V_{\Sigma^-}(t)] \right\} \\
F_{2\Sigma^-}(t) &= \left(\frac{2}{3} + \frac{1}{6}\mu_p\right) \left(\frac{1-W_{\Sigma^-}^2}{1-W_{\Sigma^-N}^2}\right)^6 \prod_{i=\rho}^{\rho''} U_i^{\Sigma^-}[W_{\Sigma^-}(t)] + \\
&+ \left(\frac{1-V_{\Sigma^-}^2}{1-V_{\Sigma^-N}^2}\right)^6 \left\{ \left(-\frac{2}{9} - \frac{1}{18}\mu_p\right) \prod_{i=\omega}^{\omega''} R_i^{\Sigma^-}[V_{\Sigma^-}(t)] + \left(\frac{2}{9} - \frac{4}{9}\mu_p\right) \prod_{i=\phi}^{\phi''} R_i^{\Sigma^-}[V_{\Sigma^-}(t)] \right\},
\end{aligned} \tag{43}$$

where

$$\begin{aligned}
U_i^B[W_B(t)] &= \frac{(W_{BN} - W_i)(W_{BN} - W_i^*)(W_{BN} - 1/W_i)(W_{BN} - 1/W_i^*)}{(W_B - W_i)(W_B - W_i^*)(W_B - 1/W_i)(W_B - 1/W_i^*)}, \quad i = \rho, \rho', \rho'' \tag{44} \\
R_i^B[V_B(t)] &= \frac{(V_{BN} - V_i)(V_{BN} - V_i^*)(V_{BN} - 1/V_i)(V_{BN} - 1/V_i^*)}{(V_B - V_i)(V_B - V_i^*)(V_B - 1/V_i)(V_B - 1/V_i^*)}, \quad i = \omega, \omega', \omega'', \phi, \phi', \phi''.
\end{aligned}$$

Each of these FF's is defined on a four sheeted Riemann surface in t -variable with the first sheet to be a physical one. Poles corresponding to vector meson resonances are placed on unphysical sheets.

Since the Körner-Kuroda model contains no free parameters and its unitarization produces also no free parameters, provided the second branch point is placed just in the baryon-antibaryon threshold, then one can predict the behaviour of all octet $1/2^+$ baryon EM FF's as it is shown in Figs.1-8. The corresponding total cross-sections of electron-positron annihilation into baryon-antibaryon, obtained by means of the expression

$$\sigma_{tot}(e^+e^- \rightarrow B\bar{B}) = \frac{4\pi\alpha^2}{3t} \left(1 - \frac{4m_B^2}{t}\right)^{1/2} [|G_M(t)|^2 + \frac{2m_B^2}{t} |G_E(t)|^2] \tag{45}$$

are presented in Figs.9-16, where they are also compared with existing data.

In Fig.9 a better agreement with low energy data on protons is achieved with unitarized Körner-Kuroda model, however, the last point from the newest measurement by the FENICE experiment in Frascati at $t=5.95$ GeV², equally the three points from the FERMILAB E760 experiment at large values of c.m. energies, are described even worse than with zero-width Körner-Kuroda model. But unitarization improved a description of the data on the cross-section of the $e^+e^- \rightarrow n\bar{n}$ process, as it is shown in Fig.10, and one experimental point on the $e^+e^- \rightarrow \Lambda\bar{\Lambda}$ process (see Fig.11) is also described quite well. There are no data on the rest of baryons of the octet $1/2^+$.

4 CONCLUSIONS AND SUMMARY

It is well known [18-20], that the investigation of polarization effects in electron-positron annihilation processes into baryon-antibaryon pairs, or in reverse processes, one can not do without complex baryon EM FF's. However, they exist up to now only for nucleons [12-14], and for the Λ -hyperon [16], to some extent. Therefore, in this paper, we have tried to remedy this shortage of the latter, at least in baryon $1/2^+$ octet.

Our problem was simplified by an existence of the elegant zero vector-meson width Körner-Kuroda model [17], which, moreover, is without any free parameters.

Since it was constructed more than one decade ago, first, we have restored the zero vector-meson width Körner-Kuroda model on a more topical physical basis. By means of the latter we have calculated as a by-product the electromagnetic mean-square radii of octet $1/2^+$ baryons. Their comparison with other model predictions indicates on a reliability of the Körner-Kuroda model [17], which stimulated us to unitarize it.

The unitarization of the Körner-Kuroda model was carried out by an incorporation of a two-cut approximation of the correct analytic properties of the octet $1/2^+$ baryon EM FF's, where the first branch point is identified with the lowest and the second one with baryon-antibaryon threshold. Finally an instability of vector-mesons was taken into account by incorporating nonzero values of vector-meson widths. In this manner every EM FF of octet $1/2^+$ baryons is defined on four sheeted Riemann surface with complex poles, corresponding to vector-meson resonances, placed on unphysical sheets.

The calculated total cross-sections of electron-positron annihilation into baryon-antibaryon processes show, that undoubtful improvement in a description of two existing FENICE points [3] on neutrons is achieved. The same can be said about the low-energy data on protons, but E760 data from FERMILAB at high values of c.m. energy are

not described neither with the zero vector-meson width Körner-Kuroda model, nor with the unitarized one. A good description is achieved also for one existing point on the Λ -hyperon.

Acknowledgments

One of the authors (S.D.) would like to thank Professor Abdus Salam, the International Atomic Energy Agency and UNESCO for hospitality at the International Centre for Theoretical Physics in Trieste. J.K. would like to thank Professor S. Fantoni for hospitality at SISSA.

References

- [1] A.Bodek: Talk presented at the VI-th Rencontres de Blois, "The Heart of the Matter" held in Blois, France, June 20-25, 1994.
- [2] A.Antonelli, R.Baldini et al: Preprint LNF-94/032 (P), Frascati (Roma) (1994)
G.Bardin et al: Nucl. Phys. B411 (1994) 3.
T.A.Armstrong et al: Phys. Rev. Lett. 70 (1992) 1212.
D.Bisello et al: Nucl. Phys. B224 (1983) 379.
- [3] A.Antonelli et al: Phys. Lett. B313 (1993) 283.
- [4] D.Bisello et al: Z. Phys. C48 (1990) 23.
- [5] T.Massam and A.Zichichi: Nuovo Cimento 43 (1966) 1137.
- [6] I.Bender et al: Nuovo Cimento A16 (1973) 377.
- [7] S.Blatnik and N.Zovko: Acta Phys. Austriaca 39 (1974) 62.
- [8] G.Höhler et al: Nucl. Phys. B114 (1976) 505.
- [9] S.Mehrotra and M.Roos: Phys. Scr. 13 (1976) 265.
- [10] P.Ceseli, M.Nigro and C.Voci: Proc. of a Workshop on Physics at Lear with Low-Energy Cooled Antiprotons, Erice, 1982, p.365.
- [11] M.Gari and W.Krúmpelmann: Phys. Lett. 141B (1984) 295.
- [12] S.Dubnička: Nuovo Cimento A100 (1988) 1, A103 (1990) 1417.
- [13] S.I.Bilenkaya, S.Dubnička, A.Z.Dubničková and P.Striženec: Nuovo Cimento A105 (1992) 1421.
- [14] S.Dubnička, A.Z.Dubničková and P.Striženec: Nuovo Cimento A106 (1993) 1253.
- [15] M.Warns, W.Pfeil and H.Rollnik: Phys. Lett. 258B (1991) 431.
- [16] A.Z.Dubničková, S.Dubnička, M.E.Biagini and A.Castro: Czech. J. Phys. 41 (1991) 1177.
- [17] J.G.Körner and M.Kuroda: Phys. Rev. D16 (1977) 2165.
- [18] A.Z.Dubničková, S.Dubnička and M.P.Rekalo: Preprint JINR, E2-92-522, Dubna (1992).
- [19] S.M.Bilenky, G.Giunti and V.Wataghin: Z. Phys. C59 (1993) 475.
- [20] J.Kraskiewicz and R.Raczka: Proc. of the 2-nd Adriatic Research Conf., "Polarization Dynamics in Nuclear and Particle Physics", Ed. A.Barut et al., World. Sci. Co., Singapore (1992).

- [21] P.Leal Ferreira, J.A.Halayel and N.Zagury: Nuovo Cimento A55 (1980) 215.
- [22] N.Barik, S.N.Jena and D.P.Rath: Phys. Rev. D41 (1990) 1568.
- [23] J.Kunz and P.J.Mulder: Phys. Rev. D41 (1990) 1578.
- [24] D.B.Leinweber, R.M.Woloshyn and T.Drapper: Phys. Rev. D43 (1991) 1659.
- [25] A.Z.Dubničková, S.Dubnička and P.Striženec: Czech. J. Phys. 43 (1993) 1177.
- [26] S.Dubnička, A.Z.Dubničková and V.Wataghin: Proc. of Hadron Structure'94 Conf., September 19-23, 1994, Košice, Slovakia.
- [27] R.G.Sachs: Phys. Rev. 126 (1962) 2256.
- [28] G.P.Lepage and S.J.Brodsky: Phys. Rev. D22 (1980) 2157.
- [29] Ch.-R.Ji, A.F.Sill and R.M.Lombard-Nelsen: Phys. Rev. D36 (1987) 165.
- [30] Review of Particle Properties: Phys. Rev. D45, Part 2, (June 1992).
- [31] M.Gourdin: Unitary Symmetries, North-Holland Publ. C., Amsterdam (1967).
- [32] O.Dumbrajs et al: Nucl. Phys. B216 (1983) 277.

Table 1. The electric mean-square radii of octet $1/2^+$ baryons predicted by the Körner-Kuroda (KK) model and their comparison with predictions following from the lattice QCD [24], the constituent quark models [21,22], the Skyrme model [23], the naive VMD model combined with SU(3) symmetry [25], the relativised quark model [15] and the extended VMD model constrained by QCD asymptotics [26].

B	$\langle r_E^2 \rangle$ [fm ²]								
	[24]	[21]	[22]	[23]	[25]	[15]	[26]	KK	Exp.[32]
p	0.426	0.870	0.664	0.775	0.508	—	0.623	0.623	0.743
n	< 0	0	0	-0.308	-0.133	-0.081	-0.128	-0.063	-0.119
Λ	> 0	0.120	0.091	0.107	0.179	0.120	-0.029	0.009	—
Σ^+	0.532	0.990	0.753	0.964	0.418	—	0.563	0.632	—
Σ^0	> 0	0.120	0.091	0.107	0.185	0.083	0.026	0.091	—
Σ^-	-0.332	-0.750	-0.570	-0.751	-0.049	—	-0.511	-0.449	—
Ξ^0	> 0	0.240	0.190	0.221	0.678	—	0.117	0.044	—
Ξ^-	-0.262	-0.630	-0.475	-0.261	-0.325	—	-0.334	-0.396	—

Table 2. The magnetic mean-square radii of octet $1/2^+$ baryons predicted by the Körner-Kuroda (KK) model and their comparison with predictions following from the lattice QCD [24], the Skyrme model [23], the naive VMD model combined with SU(3) symmetry [25], the relativised quark model [15] and the extended VMD model constrained by QCD asymptotics [26].

B	$\langle r_M^2 \rangle$			[fm ²]			Exp.[32]
	[24]	[23]	[25]	[15]	[26]	KK	
p	0.832	1.241	1.099	—	1.553	1.553	1.986
n	-0.451	-0.842	-0.763	-1.094	-1.122	-1.092	-1.458
Λ	-0.076	-0.116	0.175	-0.218	-0.421	-0.400	—
Σ^+	0.778	1.401	0.016	—	1.400	1.508	—
Σ^0	0.187	0.305	0.152	0.712	0.432	0.498	—
Σ^-	-0.416	-0.790	0.287	—	-0.535	-0.511	—
Ξ^0	-0.237	-0.605	0.967	—	-0.390	-0.895	—
Ξ^-	-0.069	0.162	-0.625	—	0.042	-0.269	—

Figure captions

- Fig.1. A prediction of the proton electric and magnetic FF's by means of the unitarized Körner-Kuroda (UKK) model and their comparison with a prediction of the zero vector-meson width Körner-Kuroda (KK) model.
- Fig.2. A prediction of the neutron electric and magnetic FF's by means of the unitarized Körner-Kuroda (UKK) model and their comparison with a prediction of the zero vector-meson width Körner-Kuroda (KK) model.
- Fig.3. A prediction of the Λ -hyperon electric and magnetic FF's by means of the unitarized Körner-Kuroda (UKK) model and their comparison with a prediction of the zero vector-meson width Körner-Kuroda (KK) model.
- Fig.4. A prediction of the Σ^+ -hyperon electric and magnetic FF's by means of the unitarized Körner-Kuroda (UKK) model and their comparison with a prediction of the zero vector-meson width Körner-Kuroda (KK) model.
- Fig.5. A prediction of the Σ^0 -hyperon electric and magnetic FF's by means of the unitarized Körner-Kuroda (UKK) model and their comparison with a prediction of the zero vector-meson width Körner-Kuroda (KK) model.
- Fig.6. A prediction of the Σ^- -hyperon electric and magnetic FF's by means of the unitarized Körner-Kuroda (UKK) model and their comparison with a prediction of the zero vector-meson width Körner-Kuroda (KK) model.
- Fig.7. A prediction of the Ξ^0 -hyperon electric and magnetic FF's by means of the unitarized Körner-Kuroda (UKK) model and their comparison with a prediction of the zero vector-meson width Körner-Kuroda (KK) model.
- Fig.8. A prediction of the Ξ^- -hyperon electric and magnetic FF's by means of the unitarized Körner-Kuroda (UKK) model and their comparison with a prediction of the zero vector-meson width Körner-Kuroda (KK) model.
- Fig.9. A prediction of the total cross-section of the $e^+e^- \rightarrow p\bar{p}$ process by means of the unitarized Körner-Kuroda (UKK) model and its comparison with a prediction of the zero vector-meson width Körner-Kuroda (KK) model and existing data. The last three points are from the E760 experiment in FERMILAB.
- Fig.10. A prediction of the total cross-section of the $e^+e^- \rightarrow n\bar{n}$ process by means of the unitarized Körner-Kuroda (UKK) model and its comparison with a prediction of the zero vector-meson width Körner-Kuroda (KK) model and the existing two experimental points from the FENICE experiment in Frascati.
- Fig.11. A prediction of the total cross-section of the $e^+e^- \rightarrow \Lambda\bar{\Lambda}$ process by means of the unitarized Körner-Kuroda (UKK) model and its comparison with a prediction of the zero vector-meson width Körner-Kuroda (KK) model and the existing one experimental point obtained by DM2 detector in ORSAY.

Fig.12. A prediction of the total cross-section of the $e^+e^- \rightarrow \Sigma^+\bar{\Sigma}^+$ process by means of the unitarized Körner-Kuroda (UKK) model and its comparison with a prediction of the zero vector-meson width Körner-Kuroda (KK) model.

Fig.13. A prediction of the total cross-section of the $e^+e^- \rightarrow \Sigma^0\bar{\Sigma}^0$ process by means of the unitarized Körner-Kuroda (UKK) model and its comparison with a prediction of the zero vector-meson width Körner-Kuroda (KK) model and the existing upper bound obtained by DM2 detector in ORSAY.

Fig.14. A prediction of the total cross-section of the $e^+e^- \rightarrow \Sigma^-\bar{\Sigma}^-$ process by means of the unitarized Körner-Kuroda (UKK) model and its comparison with a prediction of the zero vector-meson width Körner-Kuroda (KK) model. There is almost no difference between predictions of both models.

Fig.15. A prediction of the total cross-section of the $e^+e^- \rightarrow \Xi^0\bar{\Xi}^0$ process by means of the unitarized Körner-Kuroda (UKK) model and its comparison with a prediction of the zero vector-meson width Körner-Kuroda (KK) model.

Fig.16. A prediction of the total cross-section of the $e^+e^- \rightarrow \Xi^-\bar{\Xi}^-$ process by means of the unitarized Körner-Kuroda (UKK) model and its comparison with a prediction of the zero vector-meson width Körner-Kuroda (KK) model. Here is also almost no difference between predictions of both models.

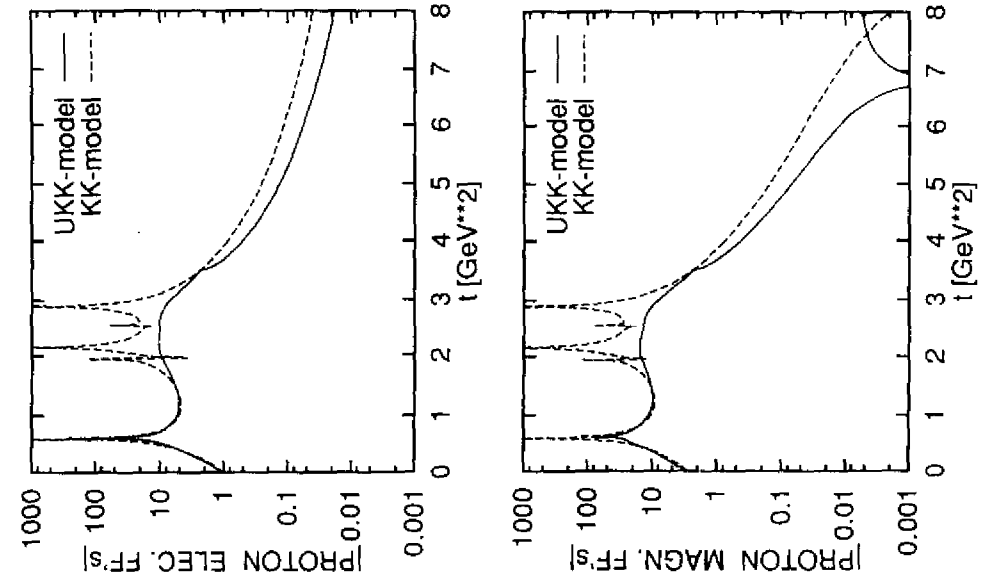


Fig.1

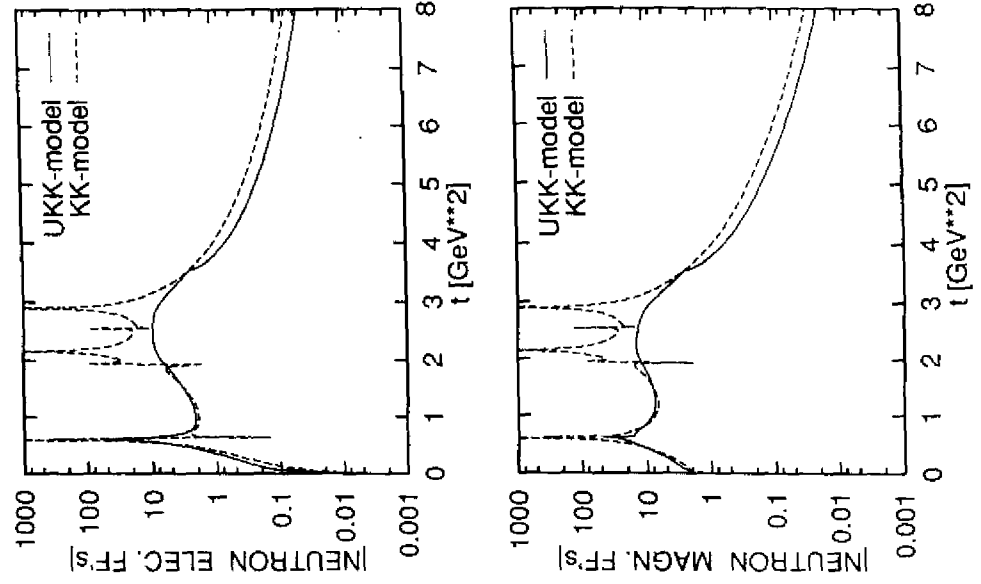


Fig.2

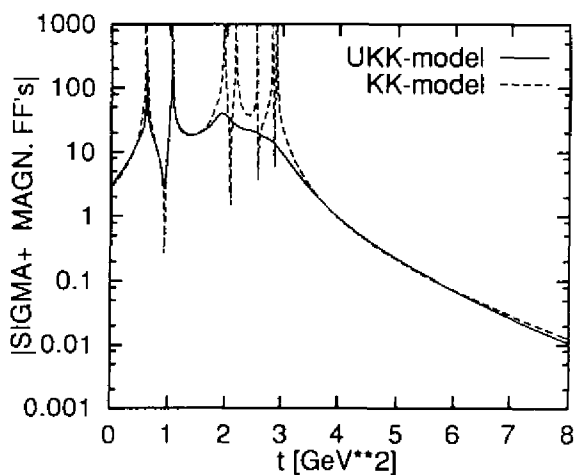
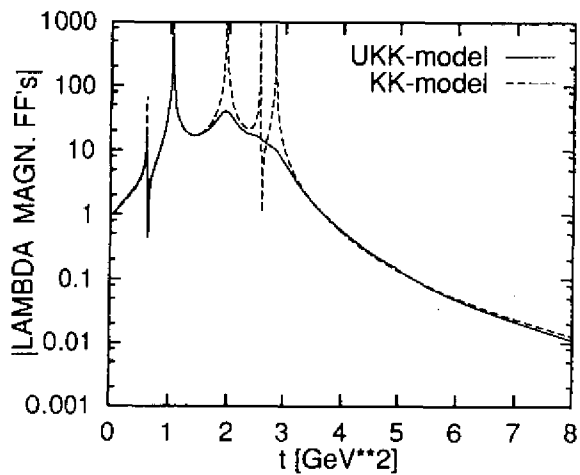
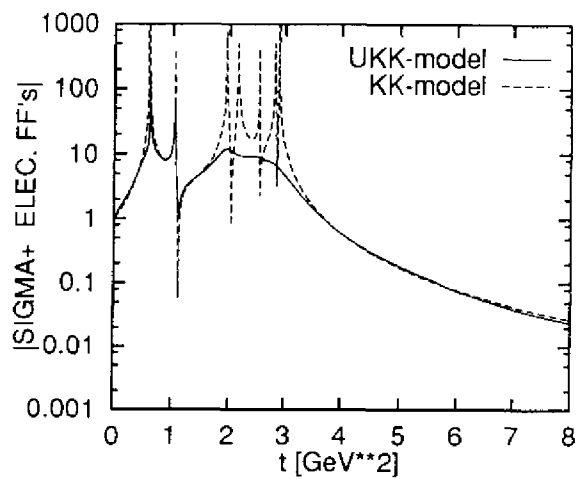
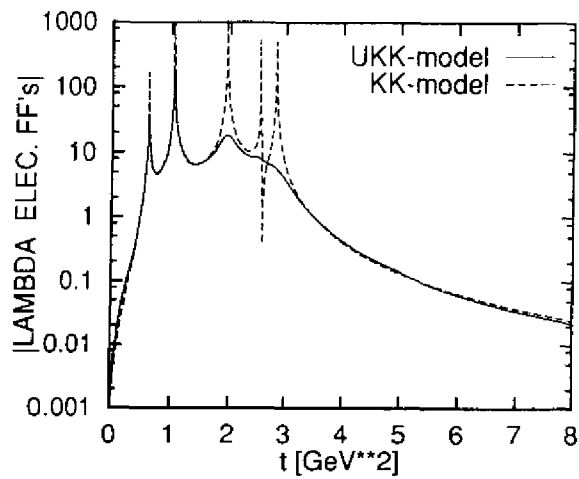


Fig.3

Fig.4

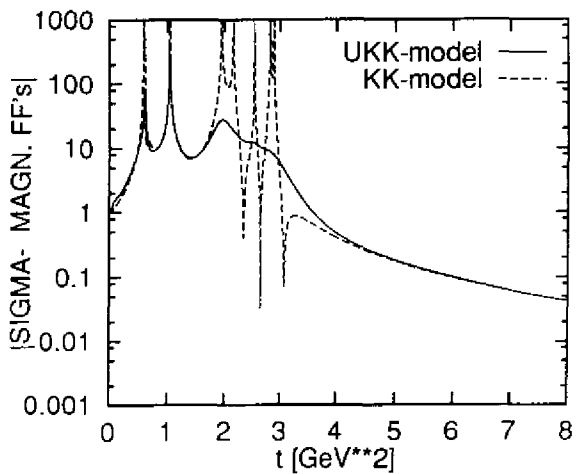
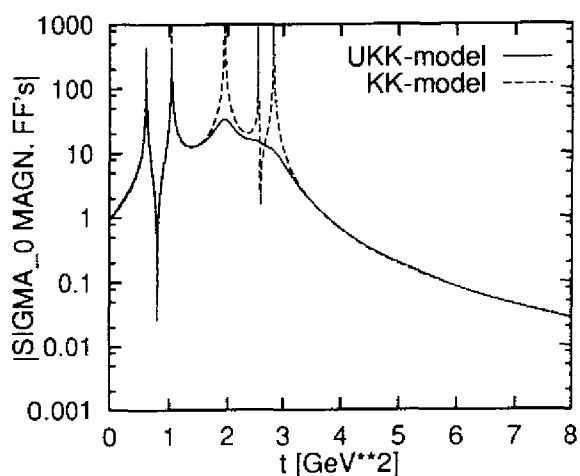
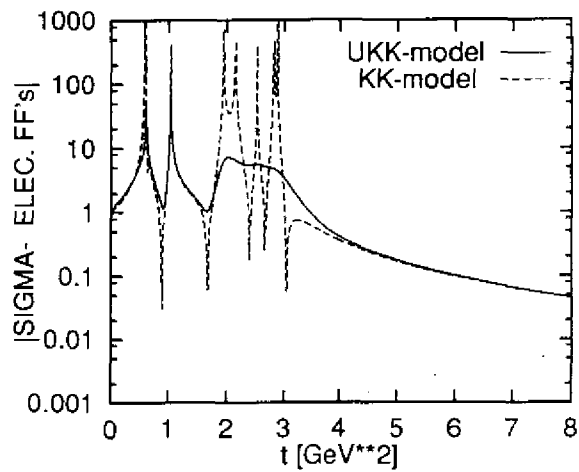
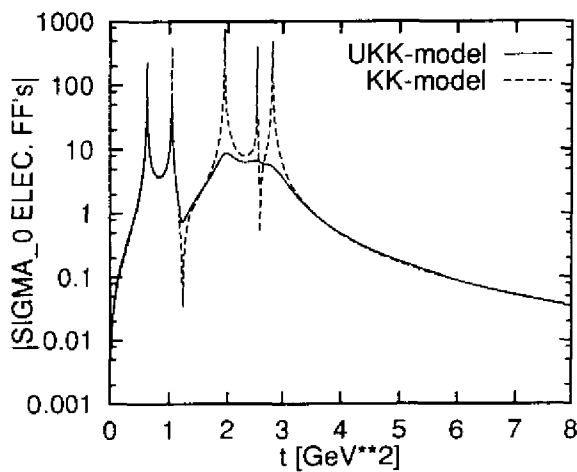


Fig.5

Fig.6

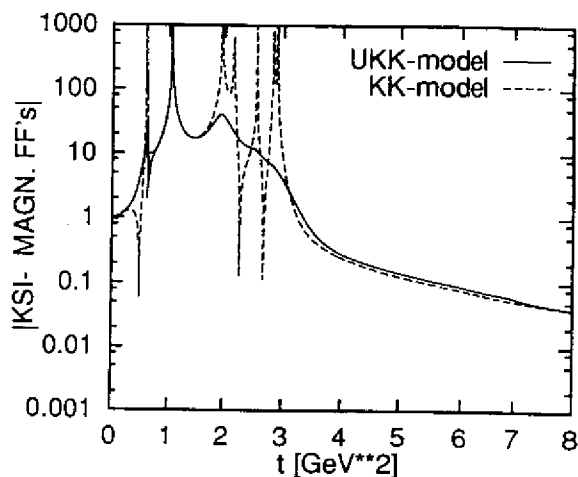
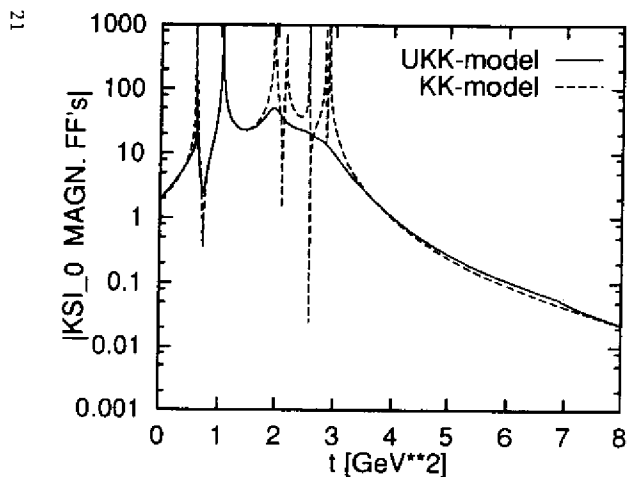
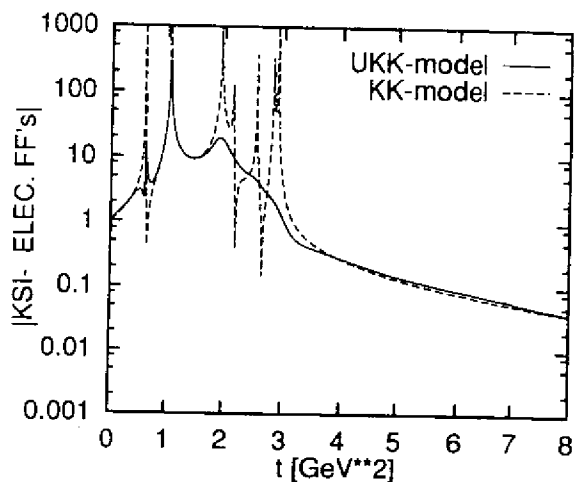
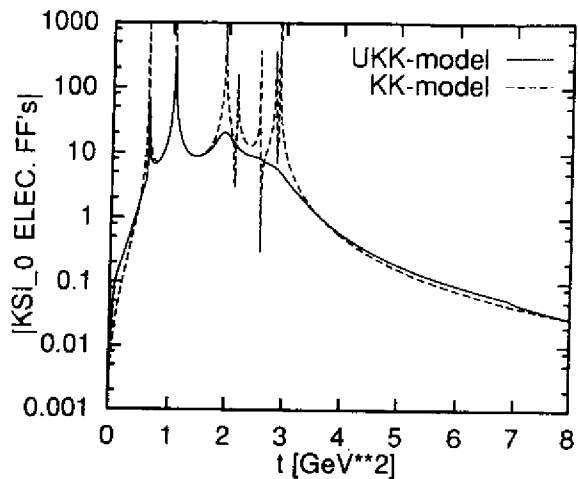


Fig.7

Fig.8

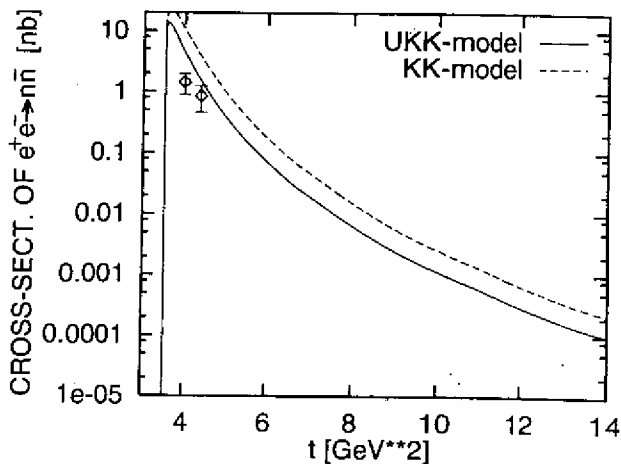
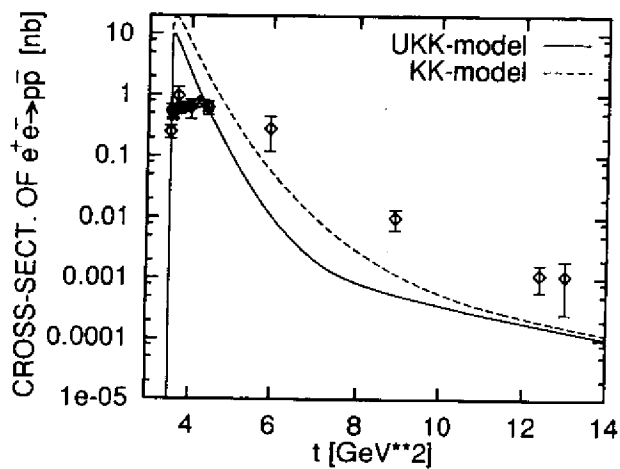


Fig.9

Fig.10

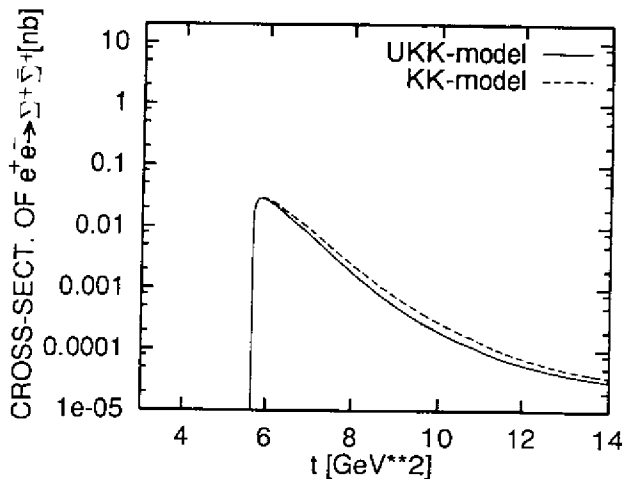
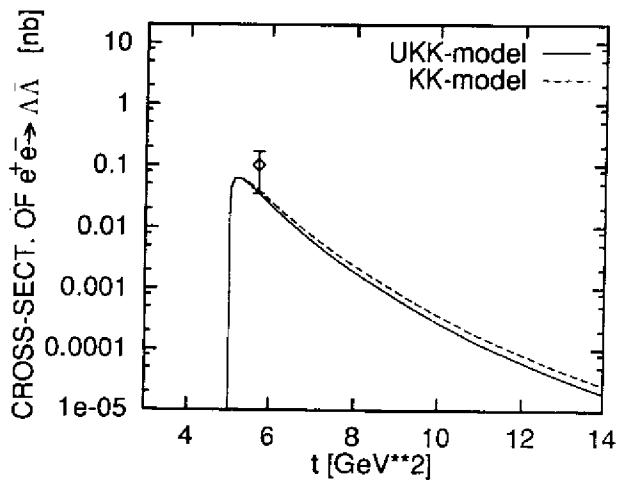


Fig.11

Fig.12

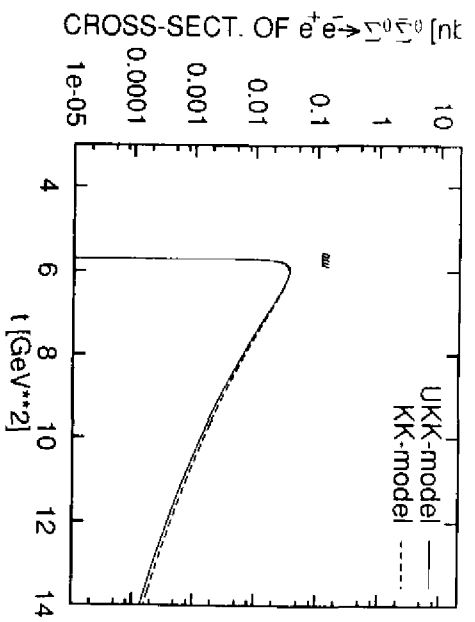


Fig.13

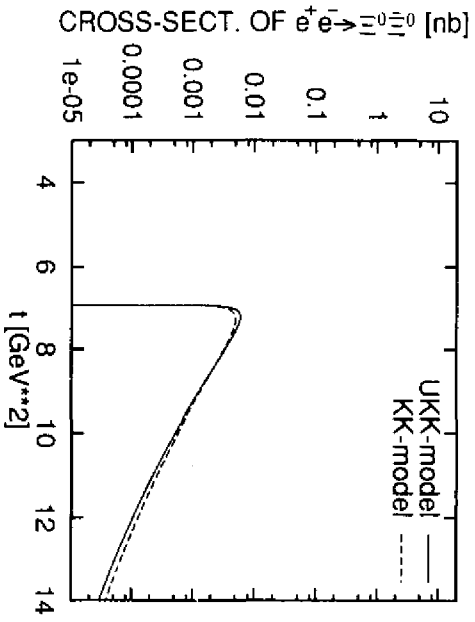


Fig.15

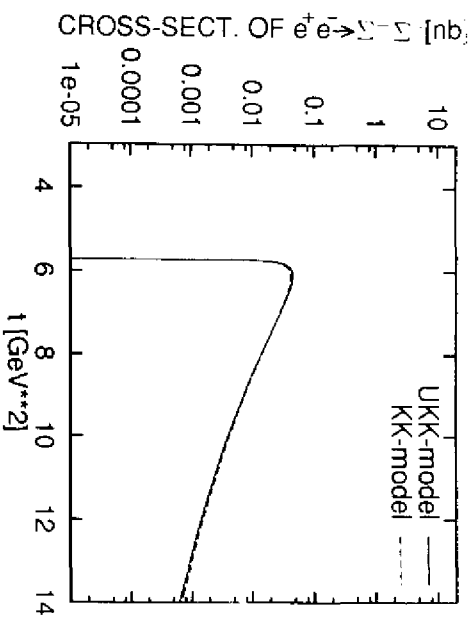


Fig.14

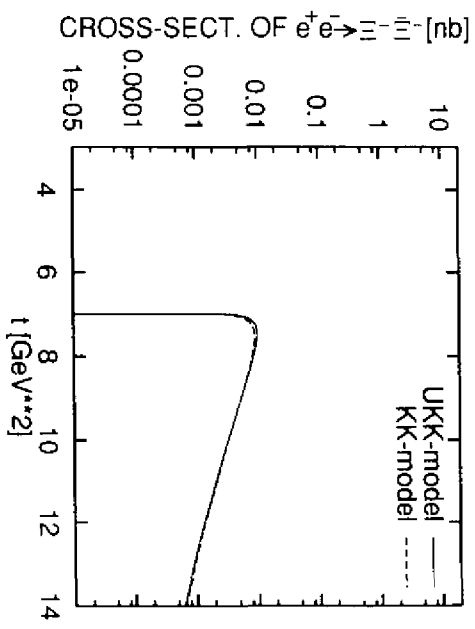


Fig.16